Chinese Journal of Physiology 55(2): 134-144, 2012
DOI: 10.4077/CJP.2012.BAA085

Effects of Phytochemicals Sulforaphane on Uridine Diphosphate-Glucuronosyltransferase Expression as well as Cell-Cycle Arrest and Apoptosis in Human Colon Cancer Caco-2 Cells

Min Wang[1], Shuo Chen[3], Shuai Wang[1], Defeng Sun[2], Jian Chen[3], Yanqing Li[3], Wei Han[3], Xiaoyun Yang[3], and Hai-qing Gao[1]

[1]*Department of Geriatrics and Gastroenterology, Qi-Lu Hospital of Shandong University Key Laboratory of Proteomics of Shandong Province; Jinan 250012*
[2]*Department of Biochemistry and Molecular Biology, Shandong Medical School, Jinan 250002 and*
[3]*Department of Gastroenterology, Qi-Lu Hospital of Shandong University, Jinan 250012 Shandong, People's Republic of China*

Abstract

Our study investigated the effects of the chemopreventive agent sulforaphane (SFN) on human colon cancer Caco-2 cells and potential underlying mechanisms of the effects. When treated with SFN at hypotoxic levels, UDP-glucuronosyltransferase 1A (UGT1A) was induced in a dose-dependent manner. SFN at 25 μM showed the highest UGT1A-induction activity, inducing UGT1A1, UGT1A8, and UGT1A10 mRNA expression, and increasing UGT-mediated N-hydroxy-PhIP glucuronidation. SFN-induced UGT1A expression may have resulted from Nrf2 nuclear translocation or activation. At higher concentrations, *e.g.* 75 μM, SFN caused G1/G2 cell cycle arrest and induced apoptosis possibly through reducing anti-apoptotic bcl-2 expression and increasing apoptosis-inducing bax expression in Caco-2 cells. Taken together, these results demonstrated the chemopreventive effects of SFN on human colon cancer Caco-2 cells may have been partly attributed to Nrf2-mediated UGT1A induction and apoptosis induction, and our studies provided theoretic and experimental basis for clinical application of SFN to human colon cancer prevention.

Key Words: Caco-2 cell line, sulforaphane, colon cancer, apoptosis, UDP-glucuronosyltransferase

Introduction

Colorectal cancer, one of the most common cancers worldwide, accounts for 9.4% of all new cancers diagnosed, with an incidence much higher in developed countries than in other parts of the world (48). Epidemiological and pharmacological studies have indicated that dietary intake of isothiocyanates through cruciferous vegetable consumption may protect against multiple cancers, including lung, stomach (47), colon (10), prostate (24), and breast (2) cancers. Sulforaphane (4-methylsulfinylbutyl isothiocyanate, SFN), a biologically active metabolite of glucoraphanin, belongs to the family of isothiocyanates and is highly enriched in cruciferous vegetables. For instance, SFN is highly expressed in the florets of

Corresponding author: Min Wang, M.D., Postdoctoral, Associate Professor, Department of Geriatrics and Gastroenterology, Qi-Lu Hospital of Shandong University, Key Laboratory of Proteomics of Shandong Province, 107 Wenhuaxi Road, Jinan 250012, Shandong, People's Republic of China. E-mail: doctorminmin@163.com
Received: November 17, 2011; Revised: January 3, 2012; Accepted: February 27, 2012.
 ISSN : 0304-4920. http://www.cps.org.tw

broccoli (7), a member of the Brassica family, and has been identified as the principal inducer of phase II detoxification enzymes in broccoli extracts (52).

Multiple mechanisms have been identified to underlie the cancer chemopreventive activities of SFN. SFN is a very potent monofunctional inducer of phase II enzymes responsible for the detoxification of procarcinogens and carcinogens, which is supported by mounting evidence from studies using cultured cells, mouse tissues (14), human intestine (28), and human airway (31). SFN-induced phase II detoxification enzymes include epoxide hydrolase, and UDP-glucuronosyltransferase (UGT) (14). SFN also inhibits cytochrome P450 (CYP) isoforms (CYP1A1, CYP2B1/2, and CYP3A4) that catalyze the activation of procarcinogens (30). In addition, SFN has been shown to inhibit cell cycle progression of prostate cancer cell line LNCaP (45) and induce apoptosis in pre-cancerous cells and tumor cells, including human glioblastoma T98G and U87MG cells (25). Moreover, SFN also inhibits the initiation of carcinogen-induced skin tumors (50) and the promotion of subcutaneous model of Barrett's esophageal adenocarcinoma *in vivo* (38), and reduces metastatic spread of melanoma in mice (46). Finally, SFN significantly enhances the antiproliferative activity of other antiproliferative agents, including paclitaxel, telomerase inhibitor MST-312, and GRN163L (38).

In addition to anticancer functions, SFN also performs antimicrobial and anti-inflammatory activities. SFN protects against numerous gram-positive and -negative bacteria (23), most notably *Helicbacter pylori* (13). SFN suppresses lipopolysaccharides-induced inflammation in mouse peritoneal macrophages (29). SFN also inhibits mRNA expression of pro-inflammatory cytokines, including TNF-α and IL-1β, as well as pro-inflammatory mediators, including Cox-2 and iNOS (29).

UGTs, a representative member of phase II detoxification enzymes, include two families: UGT1A and UGT2. As a superfamily of endoplasmic reticulum membrane bound enzymes, UGTs catalyze the addition of a β-glucuronic acid moiety to a variety of nucleophilic sites within xenobiotics and endogenous compounds and are involved in the metabolism of bilirubin, steroids, bile acids, and drugs. In addition, UGTs metabolize carcinogens, an important process for the bioinactivation and subsequent excretion of these toxic compounds. UGT-catalyzed glucuronidation is thought to account for up to 35% of phase II reactions (12). The liver is the major site of glucuronidation, and the intestine has also been reported to contain significant glucuronidation capacity. UGT1A8 and UGT1A10 have been identified as specifically expressed in the human intestine (49).

UGTs can be induced by dietary compounds in the human colonic adenocarcinoma cell line Caco-2 (1). This is an important discovery since different from most other inducers of UGTs, which are highly toxic chemicals and are thus not suitable for cancer treatment, relative low toxicity of SFN provides a promising strategy to combat carcinogenesis or cancer development.

Earlier reports have also shown that SFN induces apoptosis in prostate, bladder, leukemia, and colon cancers (3). However, little is known about the biological activity of SFN in human colon Caco-2 cells. In the current study, we examined the effects of SFN treatment on Caco-2 cells and investigated the underlying mechanisms.

Materials and Methods

Materials and Reagents

SFN (Sigma, St. Louis, MO, USA) was dissolved in dimethyl sulfoxide (DMSO) at a concentration of 1 μmol/ml and stored at -20°C to further use. 2-amino-1-methyl-6-phenylimidazo [4, 5-b] pyridine (PhIP) was a kind gift from Professor Dongxin Lin (Institution of Tumor, Peking Union Medical College, Chinese Academy of Medical Sciences, Beijing, PRC). 2-hydroxyamino-1-methyl-6-phenylimidazo [4, 5-b] pyridine (N-hydroxy-PhIP) was synthesized from its precursor PhIP by Chemistry College of ShanDong University (Jinan, Shandong, PRC).

Cell Culture

The Caco-2 human colon adenocarcinoma cells (obtained from Institute of Cytobiology, Chinese Academy of Sciences, Shanghai, PRC) were maintained as monolayers in Dulbecco's Modified Eagle Medium (DMEM) (Gibco, Rockville, MD,USA) containing 10% heat-inactivated fetal calf serum, 100 U/ml penicillin, and 100 μg/ml streptomycin at 37°C in a humidified incubator with 5% CO_2. Cells in logarithmic growth phase were used for experiments. Caco-2 cells cultured in DMEM or DMEM supplemented with DMSO, the solvent of SFN, at experimental concentrations were compared and no difference was observed, suggesting that DMSO at experimental concentrations was nontoxic to Caco-2 cells.

Cell Viability Assay

The viability of Caco-2 cells after SFN treatment was assessed using the thiazolyl blue tetrazolium bromide (MTT) assay (20). MTT (Sigma) was dissolved in PBS at 5 mg/ml. Caco-2 cells were seeded in 96-well microtiter plates, 8×10^3 cells per well in 200 μl. SFN was added at different final

concentrations (10-100 μM) in sextuplicate. Fifty microlitre MTT (5 mM) was added at 12, 24, 36, 50, 60, or 72 h, respectively. Two control groups were included: one without SFN treatment and one without cells. The optical density (OD) was measured at 570 nm in a microplate reader. The inhibition rate (IR) of cell growth was calculated as: IR = (the OD value of controls – the OD value of experimental groups) / the OD value of controls. IC50 (50% inhibitory concentration) values were also calculated using Statistic Probit software.

Western Blot

To examine whether SFN induces UGT1A, Caco-2 cells were treated with SFN for 24 h at 0, 10, 15, 20, 25, or 30 μM, and were then washed twice in ice-cold phosphate buffered saline (PBS) and lysed in complete cell lysis buffer (50 mM Tris-HCl, pH 7.4, 150 mM NaCl, 1% Triton X-100, 0.25% Na-deoxycholate, 1 mM EDTA, 1 mM NaF, 1 mM DTT, 1 mM PMSF, 1 mM activated Na_3VO_4, 1 μg/ml aprotinin, 1 μg/ml leupeptin, and 1 μg/ml pepstatin). Protein concentration in cell lysate was determined using the BCA assay. Proteins were resolved on 10% SDS-PAGE and transferred to nitrocellulose membranes. The membranes were blocked in 5% nonfat dry milk containing 0.1% Tween-20 at room temperature for 1 h, and then probed with a primary antibody against UGT1A (1:1000; Gentest, Woburn, MA, USA) at 4°C overnight. After washing, the membranes were incubated with horseradish peroxidase (HRP)-conjugated secondary antibody (1:5000; Boster, Wuhan, Hubei, PRC). The bands were detected by enhanced chemiluminescence (ECL). The intensities of acquired bands were measured by computerized image analysis system (bandscan 5.0 Demo) and normalized to β-actin as the endogenous control.

Quantitative Real-Time RT-PCR (qRT-PCR).

Caco-2 cells were treated for 24 h with SFN at the 25 μM, and total RNA was isolated from the cells by using TRIzol reagent (Invitrogen, Carlsbad, CA, USA) according to the manufacturer's protocol. Reverse transcriptase reactions were carried out with 1 μg RNA, oligo-dT15 primer and M-MLV reverse transcriptase (Toyobo, Kita-ku, Osaka, Japan) in a volume of 20 μl. The presence of UGT1A1, UGT1A8 and UGT1A10 transcripts were analyzed by qRT-PCR, based on general fluorescence detection with SYBR Green (Toyobo), using the Lightcycler2.0 (Roche, Nutley, NJ, USA). Levels of the housekeeping gene β-actin were used as an internal control for the normalization of RNA quantity and quality differences in all samples. The real-time PCR reaction conditions were 30 s at 95°C followed by 45 cycles of 5 s at 95°C, 10 s at 58°C and 15 s at 72°C. Measurements were performed in triplicates. The relative amount of mRNA was calculated as the ratio between the target mRNA and the corresponding endogenous control β-actin.

Table 1. Primer sequences for quantitative real-time RT-PCR

Gene name	Primer sequences (5' → 3')
UGT1A1	Forward: GTCCCACTTACTGCACAACAAG Reverse: GGGTCCGTCAGCATGACATCA
UGT1A8	Forward: GTTGATGCCTGTGCGTTAATTGT Reverse: GGGCAACCTATTCCCCTGGC
UGT1A10	Forward: GGCCCCGTTCCTTTATGTGTGT Reverse: GATCTTCCAGAGTGTA CGAGGTT
β-actin	Forward: GCATGTACGTTGCTATCCAGGC Reverse: GCTCCTTA ATGTCACGCACGAT

Gene-specific primers used were derived from PrimerBank and are summarized in Table 1. All primers were synthesized by BioSune (Shanghai, PRC) after accomplishing BLAST alignment in NCBI. Gene-specific amplifications were demonstrated by analyzing qRT-PCR products bands in agarose gel electrophoresis and melting curve data.

High-Performance Liquid Chromatography (HPLC)

UGT1A enzyme activity was detected by HPLC. Mass spectrometric identification of N-hydroxy-PhIP metabolites formed by UGT1A was conducted as previously described (1). Microsomal proteins (100 μg) from 25 μM SFN-treated groups or controls were analyzed by using a symmetry 5 μ C18 column (4.6 × 250 mm) (Waters, Milford, MA, USA) with UV detection at 310 nm. The mobile phase was a linear gradient of 25-100% methanol (5-40 min) at a flow rate of 1 ml/min. N-hydroxy-PhIP at 0.36 mM standard concentration was used as a control. Measurements were performed in triplicates.

Nrf2 Nuclear Translocation Analysis

Caco-2 cells in logarithmic growth phase were plated at low density (2×10^5 cells/well) on sterile glass slides in a 6-well plate and grown in monolayer. Cells were treated with 15, 25, or 35 μM SFN for 24 h before harvesting. After fixation, permeabilization, and blocking (33), cells were first immunostained with the rabbit anti-Nrf2 polyclonal antibody (1:50; Santa Cruz Biotechnology, Santa Cruz, CA, USA) and then with Cy3-labeled goat anti-rabbit (1:100; Sigma). Immunofluorescence images were acquired

using a confocal laser microscope (Zeiss, Heidenheim, Germany) with a 40 × objective (543 nm excitation and 560 nm emission).

Inverted Phase Contrast Microscopy

Caco-2 cells were untreated or treated with SFN at 75 µM for 24 h. An inverted phase contrast microscope (Olympus, Shinjuku-ku, Tokyo, Japan) was used to observe the growth and change of cells every 12 h.

Scanning Electron Microscopy

Caco-2 cells were plated on 24-well microslides and treated with control or SFN-supplemented medium at 25, 50, 75, and 100 µM for 24 or 36 h. At the end of each incubation time, samples were fixed with 2.5% glutaraldehyde in 0.1 M cacodylate buffer (pH 7.4), and post-fixed with 1% osmium tetroxide-1.5% potassium for 1 h. After dehydration with an alcohol gradient, the samples were immobilized by a conductive adhesive and sprayed with carbon and gold. Surface structure of the samples was visualized by scanning electron microscopy (Jeol, Akishima, Tokyo, Japan).

Flow Cytometry

Flow cytometry was performed as described previously (15). Briefly, Caco-2 cells were cultured in 75 cm^2 flasks at a density of 5×10^4/ml for 48 h. Cells were treated with control or SFN (25, 50, 75, and 100 µM) for 24 h and were stained by adding 0.5 ml of solution containing povidone iodine (10 µg/ml). Cell proliferation was evaluated by measuring cell cycle percentages using a FACScan flow cytometer (BD Biosciences, Woburn, MA, USA). Debris was eliminated by gating on peak versus integrated signals.

In Situ *Hybridization*

Cells were plated at a density of 5×10^4/ml on sterile glass cover slides in a 6-well plate and treated with control (DMSO) or 75 µM SFN for 24 h. After cells were fixed in methanol (-20°C, 20 min), endogenous peroxidase activity was blocked by 3% H_2O_2 for 8 min and the cells were stained with 3% pepsin diluted in citric acid, 0.5 M PBS, and distilled water. Hybridization was performed overnight in a calorstat by adding 20 µl of hybridization solution containing oligonucleotide probes of bcl-2 and bax (Boster). Slides was washed and subjected to confining liquid prior to the addition of biotinylated rat anti-digoxin antibodies SABC (Boster). Then slides were rinsed with PBS and stained with DAB. Expression of bcl-2 and bax mRNA was detected in a light microscope and analyzed using Tiger computerized image analysis system in five randomly selected fields from each cover slide.

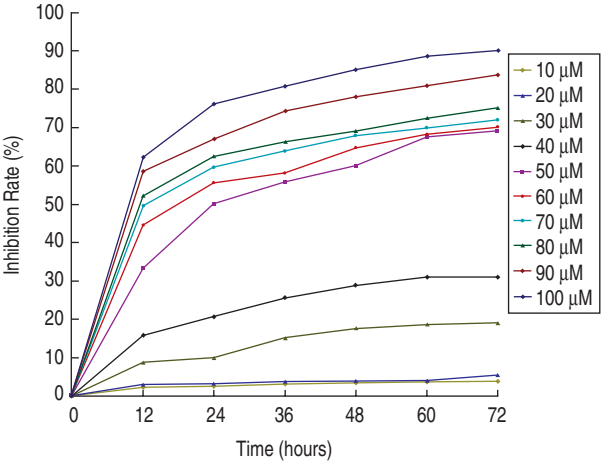

Fig. 1. **High concentrations of SFN inhibit Caco-2 cell growth and viability.** Caco-2 cells were treated with increasing concentrations of SFN. Cell viability was measured at various time points using the MTT assay. Results are expressed as inhibition rate (%) and are representative of three independent experiments.

Statistical Analyses

Statistical analysis was performed using Statistical Package for the Social Sciences 13.0 (SPSS 13.0). Data were presented as means ± SD. Differences among different treatment groups were analyzed using Student's *t*-test or one-way analysis of variance (ANOVA). Differential analysis for continuous variables was performed with Pearson correlations. A *P*-value < 0.05 was considered statistically significant.

Results

Cytotoxicity of SFN on Colon Cancer Cell Growth

To study the antitumor effects of SFN on colon cancer Caco-2 cells, we first examined the cytotoxicity of SFN on cell growth. Compared with controls, SFN, starting from 30 µM, inhibited Caco-2 cell growth and this inhibition was dose- and time-dependent (Fig. 1). The influence on cell growth and adherence was already significant at 50 µM, the IC50, and, thus, this and lower concentrations below were used in further experiments.

SFN Increases UGT1A Protein Expression in Caco-2 Cells

The UGT1A protein levels in Caco-2 cells with

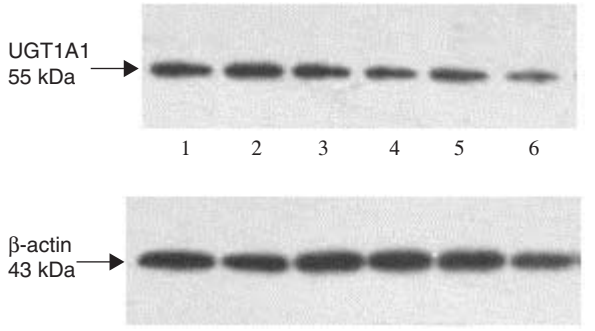

Fig. 2. **SFN induces UGT1A protein expression in Caco-2 cells.** Induction of UGT1A protein after treated with SFN at various concentrations for 24 h. Cells were treated with SFN at 30 μM (lane 1), 25 μM (lane 2), 20 μM (lane 3), 15 μM (lane 4), 10 μM (lane 5), and 0 μM (control, lane 6). The gel shown is representative of three independent experiments.

or without SFN treatment were compared. Western blot analysis showed that after the cells were treated with SFN for 24 h at relatively low toxic concentrations (10-30 μM), UGT1A protein expression increased with SFN concentration (Fig. 2). SFN at 25 μM displayed the greatest induction effect (lane 2, Fig. 2).

SFN Induces UGT1A1, UGT1A8 and UGT1A10 mRNA Expression in Caco-2 Cells

We further examined whether SFN could induce expression of the UGT1A isoforms UGT1A1, UGT1A8, and UGT1A10 by qRT-PCR. Based on the results of Western blot analysis, we chose 25 μM SFN to treat Caco-2 cells for 24 h. The mRNA levels of all three isoforms were significantly higher in 25 μM SFN-treated samples than in controls (Fig. 3A). The qRT-PCR products were analyzed by agarose gel electrophoresis, and they were confirmed to be a single band of the expected size (Fig. 3B).

SFN Induces N-hydroxy-PhIP Glucuronidation in Caco-2 Cells

A prediction of increased UGT1A levels is an increase in the level of UGT-catalyzed glucuronidation. To test this, we examined whether SFN induced UGT-mediated N-hydroxy-PhIP glucuronidation by HPLC/MS. As a control, microsomes from untreated cells were incubated with 0.36 mM N-hydroxy-PhIP for 1 h. This incubation produced a minor HPLC peak with a retention time of 8 min (Fig. 4Aa). HPLC/MS analysis of this peak demonstrated an $[M+H]^+$ ion of m/z 417, consistent with a glucuronic acid conjugate of N-hydroxy-PhIP (32). Upon collision-induced dissociation, product ions of m/z 241 were observed, indicative of N-hydroxy-PhIP. The UV absorption maximum for

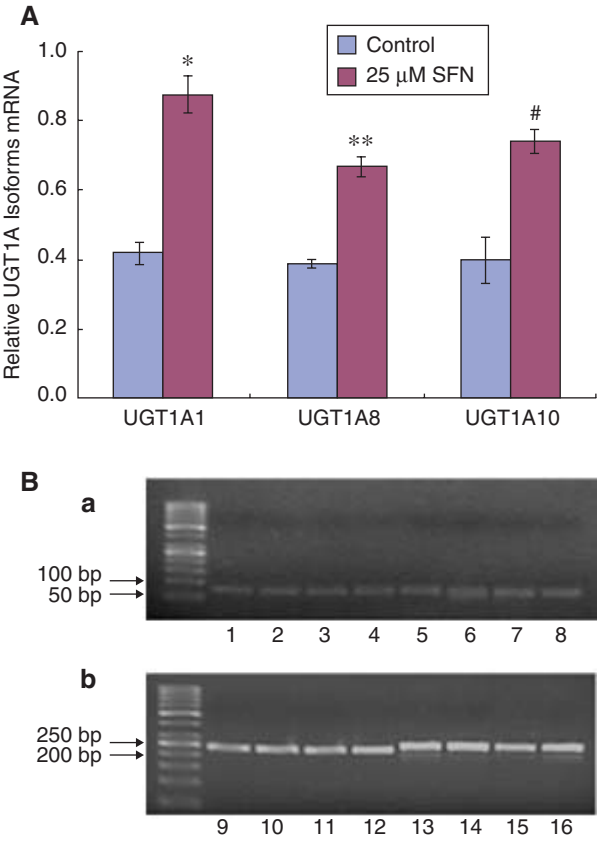

Fig. 3. **SFN induces UGT1A1, UGT1A8, and UGT1A10 mRNA expression in Caco-2 cells.** [A] Induction of UGT1A1, UGT1A8, and UGT1A10 mRNA expression in Caco-2 cells treated with 25 μM SFN for 24 h. They were analyzed in a qRT-PCR assay relative to corresponding endogenous control β-actin. Experiments were performed in triplicates. (Significant difference compared with control group respectively, $*P = 0.006$, $**P = 0.017$, $^{\#}P = 0.008$) [B] The quantitative real-time RT-PCR products were analyzed by electrophoresis through agarose gels and viewed under UV light after ethidium bromide staining. They were confined to a single band of the expected size. (a) Bands in lanes 1 to 4 are the amplified products of UGT1A1, the amplicon size is 76 bp; bands in lanes 5 to 8 are the amplified products of UGT1A8, the amplicon size is 77 bp. (b) Bands in lanes 9 to 12 are the amplified products of UGT1A10, the amplicon size is 233 bp; bands in lanes 13 to 16 are the amplified products of β-actin, the amplicon size is 250 bp.

N-hydroxy-PhIP was shifted to 319 nm in the metabolite, characteristic of N-hydroxy-PhIP-N2-glucuronide as opposed to N-hydroxy-PhIP-N3-glucuronide (32). When microsomes from SFN-treated Caco-2 cells were incubated with N-hydroxy-PhIP, there was a markedly increased peak at the expected retention time of 8 min for N-hydroxy-PhIP-N2-glucuronide (Fig. 4Ab). In three independent experiments, an average of 3-fold increase was observed in the glucuronidation of N-

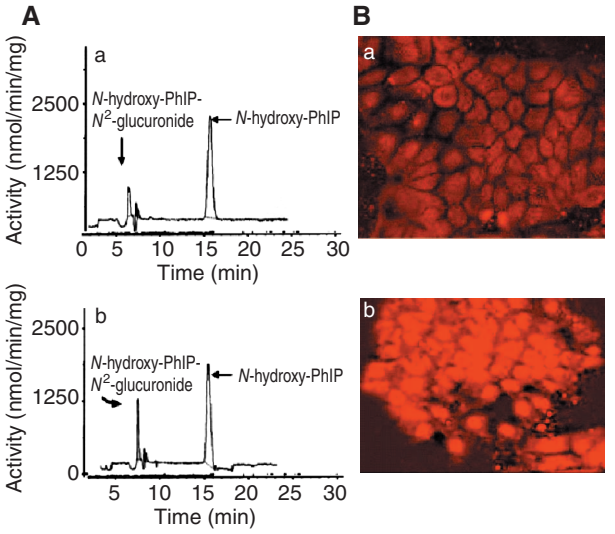

Fig. 4. **SFN induces UGT-catalyzed N-hydroxy-PhIP glucuronidation and Nrf2 nuclear translocation.** [A] Comparison of N-hydroxy-PhIP glucuronidation by microsomes from untreated Caco-2 cells (a) or microsomes from Caco-2 cells pretreated with 25 μM SFN for 3 days (b) by HPLC. The first radioactive peak (retention time ~8 min) corresponds to N-OH-PhIP-N2-glucuronide whereas the second peak (retention time ~16 min) corresponds to N-hydroxy-PhIP. Comparison of the first peak in Figs. 4A, a and b show that SFN-induced UGT increases N-hydroxy-PhIP glucuronidation. [B] Induction of nuclear translocation of Nrf2 by SFN. Immunofluorescence images (×400) of untreated control cells (a) or cells treated with 25 μM SFN for 24 h (b) are shown.

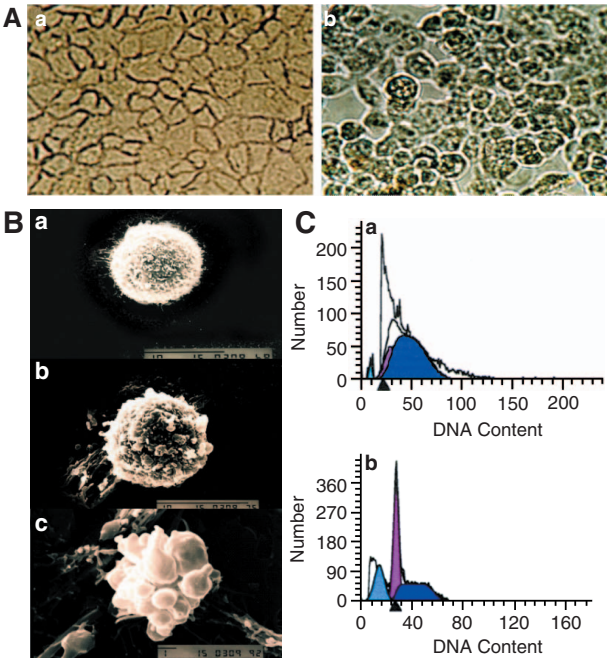

Fig. 5. **SFN induces apoptosis and arrests Caco-2 cells in G0/G1 phase.** [A] The inverted phase-contrast microscopy images of SFN-treated Caco-2 cells (×400). Caco-2 cells were treated with 0 (a) or 75 μM (b) SFN for 24 h. [B] SFN-treated Caco-2 cells underwent apoptosis as observed under scanning electron microscopy. Cells were untreated for 24 h (a, ×3500), treated with 75 μM SFN for 24 h (b, ×5000), or with 75 μM SFN for 36 h (c, ×7500). [C] Effects of SFN on cell cycle. Cells were untreated (a) or treated with 75 μM SFN for 24 h (b) and then stained with povidone iodine for DNA content analysis by flow cytometry.

hydroxy-PhIP in the SFN-treated cells as compared with the untreated Caco-2 cells.

SFN Induces Nrf2 Nuclear Translocation in Caco-2 Cells

The transcription factor Nrf2 plays an important role in antioxidant responses and has been shown to induce the expression of UGT1A isoforms (33). Therefore, we examined whether SFN could induce Nrf2 nuclear translocation and activation in Caco-2 cells. In untreated control cells, Nrf2 only showed cytoplasmic but not nuclear staining (Fig. 4Ba). In contrast, intense nuclear labeling was observed in SFN-stimulated Caco-2 cells (Fig. 4Bb). In addition, a dose-dependent increase in the Nrf2 levels after SFN treatment at 15, 25, and 35 μM was observed (data not shown).

Morphological and Ultrastructural Changes in SFN-Stimulated Caco-2 Cells

To determine whether SFN induces cell death by apoptosis or necrosis, Caco-2 cells were incubated with SFN at concentrations equivalent to one-half of the IC50, the IC50 (50 μM), 1.5-fold the IC50, and twice the IC50. Cells were imaged using inverted phase contrast microscopy (Fig. 5A). Untreated cells firmly attached to each other in an organized monolayer (Fig. 5Aa). Cells, which contained some granules in the cytoplasm, appeared oval, polygonal or irregular in shape (Fig. 5Aa). Caco-2 cells treated with 25 μM SFN looked normal and grew well. However, changes were observed after 24-h treatment of 50, 75, or 100 μM SFN. After treatment with 75 μM SFN for 24 h, cells became round with decreased size and shrunk plasma membrane (Fig. 5Ab). Cells also showed increased granules and vacuoles in the cytoplasm (Fig. 5Ab). With an increase in SFN concentration or incubation time, a net decrease in the total number of cells and an accumulation of cells floating in the culture medium were observed (data not shown).

Under scanning electron microscopy, most Caco-

Table 2. Cell cycle percentages and apoptotic rate of Caco-2 cells

	Apoptotic rate	G0/G1	S	G2/M
Control	3.20 ± 0.21	20.72 ± 0.39	76.39 ± 1.05	2.89 ± 0.68
25 μM SFN	4.16 ± 0.29	37.86 ± 1.12*	60.12 ± 1.75	2.02 ± 0.68
50 μM SFN	15.68 ± 1.06*	35.45 ± 1.54**	44.66 ± 2.56	19.89 ± 1.25
75 μM SFN	26.79 ± 1.75*	56.17 ± 1.80**	43.56 ± 1.25	0.27 ± 0.15
100 μM SFN	13.65 ± 2.74*	60.78 ± 2.15**	38.12 ± 0.56	1.10 ± 0.75

Cells were untreated or treated with SFN at the indicated concentrations for 24 h. Results are expressed as means ± SD of three independent experiments.
*$P < 0.05$; **$P < 0.01$. Apoptotic rate = the number of apoptotic cells/total tested cells × 100%.

2 cells were rich in microvilli on the surface (Fig. 5Ba). The same results were observed in cells treated with 25 μM for 24 h (data not shown). In contrast, in cells treated with SFN for 24 h at 50 (data not shown) or 75 μM (Fig. 5Bb), microvilli became short and globular, and cells became small and round with wide intercellular space. Cells showed typical characteristics of apoptosis: namely cell detachment, membrane blebbing, cell shrinkage with a condensed cytoplasm, vesicle formation (abundant vacuoles with multivesicular bodies), and apoptotic bodies (Fig. 5Bb). When the SFN treatment (75 μM) was extended to 36 h (Fig. 5Bc) or longer (data not shown), changes of the dying cells were more typical and obvious.

SFN Treatment Results in Arrests of Caco-2 Cells in G0/G1 Phase and Induction of Apoptosis

Cell cycle of SFN-treated Caco-2 cells was examined at concentrations equal to one-half of the IC50, the IC50 (50 μM), 1.5-fold the IC50, and twice the IC50 (Table 2 and Fig. 5C). Most untreated cells (76.39 ± 1.05%) were in the S phase due to the high proliferative state of this cell line. In contrast, an increase in the G0/G1 phase cells was observed in the presence of 25 μM ($P < 0.05$), 50 μM ($P < 0.01$), 75 μM ($P < 0.01$), or 100 μM ($P < 0.01$) SFN throughout the entire 24 h treatment (Table 2). These results suggested that the G0/G1 phase accumulation was caused not only by an increase in the duration of the G0/G1 phase but also by a complete arrest of many cells in the G0/G1. The G0/G1 phase accumulation was accompanied by a decrease in the percentage of cells in the S phase. Interestingly, flow cytometry analysis showed the presence of a sub-G1 peak characteristic of potential apoptotic cells [apoptotic rate (AR) = 3.20 ± 0.21%] in untreated cells, which indicated that spontaneous apoptosis existed. The percentage of apoptotic cells in 25 μM SFN-treated cells was not significantly different from that of untreated cells ($P = 0.064$). However, the ratio of apoptotic cells with subdiploid DNA content significantly increased in 50 μM ($P < 0.05$), 75 μM ($P < 0.05$), and 100 μM ($P < 0.05$) SFN-stimulated cells at 24 h (Table 2). The AR of 100 μM SFN-treated cells was less than that of 75 μM-treated cells, possibly due to cell necrosis.

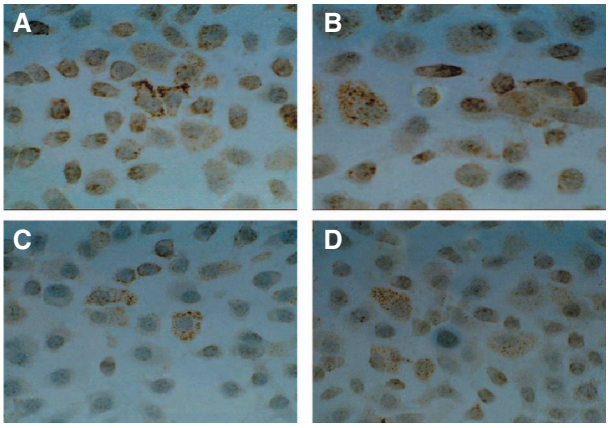

Fig. 6. **SFN affects the expression levels of bcl-2 and bax mRNA.** Caco-2 cells were treated without or with 75 μM SFN for 24 h, analyzed by *in situ* hybridization for bcl-2 and bax mRNAs, and imaged by a light microscope (×400). A: untreated cells, bcl-2 mRNA; B: untreated cells, bax mRNA; C: 75 μM SFN-treated cells, bcl-2 mRNA; D: 75 μM SFN-treated cells, bax mRNA.

SFN Increases bcl-2 and Decreases Bax mRNA Expression in Caco-2 Cells

To study the potential mechanisms of SFN-induced apoptosis, we examined how SFN treatment would affect the mRNA expression levels of bcl-2, which is an anti-apoptotic regulator, and bax, an apoptosis inducer. Untreated Caco-2 cells showed strong signals of bcl-2 mRNA and weak signals of bax mRNA (Figs. 6, A and B). In contrast, 75 μM SFN treatment for 24 h significantly decreased bcl-2 mRNA expression ($P = 0.003$) and increased bax mRNA expression level ($P = 0.006$) (Table 3 and Figs. 6, C and D).

Table 3. Influence of SFN on the expression of bcl-2 and bax mRNA

	bcl-2 mRNA	bax mRNA
Control	0.146 ± 0.009	0.088 ± 0.035
75 μM SFN	0.015 ± 0.009*	0.302 ± 0.057**

Low-power (×40) and high-power (×400) images of *in situ* hybridization were analyzed by the Tiger computerized image analysis system. Results are expressed as means ± SD of five randomly selected fields.
*P = 0.003; **P = 0.006.

Discussion

In our previous studies (40), we observed decreases in the expression and activities of UGTs in the epithelium of colorectal tissues in comparison with the normal samples. In this study, we cultured the human colon cancer cell line Caco-2 with SFN and showed that the expression of UGT1A protein could be induced in a dose-dependent manner when treated with 10-30 μM SFN for 24 h and this induction by SFN was most powerful at 25 μM (Fig. 2). We also confirmed that the induced UGT1A was functional as shown by the increased glucuronidation of N-OH-PhIP under SFN treatment (Fig. 4A). Our data are consistent with several previous reports on the effects of SFN treatment on other cancer cell types. For example, dihydrodiol dehydrogenase and aldo-keto reductase are induced in both the human colon LS-174 adenocarcinoma cell line and SV40 immortalized human colon epithelial cells (5). UGT1A1 and GSTA1 are induced in both human colon cancer HT-29 cells and hepatoma carcinoma cell line HepG2 (4). In contrast to our study, Petri *et al*. reported that SFN alone induced GST (3.1-fold) but not UGT in differentiated Caco-2 cells whereas another antioxidant, quercetin, which is a plant-derived flavonoid, induced UGT (up to 2.6-fold) but not GST by itself (37). This contradiction may have resulted from different durations of treatment (24 h *vs.* 2 h), different SFN concentrations (25 μM *vs.* 10 μM), or the low basal levels of GST in Caco-2 cells (4).

We further showed that SFN induced UGT1A1 mRNA, which is extensively expressed in various human tissues, and UGTlA8 and 1A10 mRNAs, which are exclusively expressed in human intestinal mucosa (Fig. 3A). To our knowledge, this is the first report demonstrating the ability of SFN to induce UGTlA8 and UGT1A10 mRNAs in Caco-2 cells. We were not able to examine the protein levels and individual activities of these three isoforms due to the lack of specific antibodies. The pattern of glucuronide formation is different between UGT isoforms. The significant increase in the peak of N-OH-PhIP-N2-glucuronide observed in our study (Fig. 4A) is consistent with previous findings that UGT1A1, UGT1A8, and UGT1A10 all predominantly produce N-OH-PhIP-N2-glucuronide (32, 36). Expression of UGT isoforms in the colon leads to the reconjugation of hydrolyzed N-OH-PhIP and this reaction has been shown to induce UGT activities (34). Therefore, it is possible that some of the observed increase in N-OH-PhIP-N2-glucuronide formation may be due to the induction of UGT by N-OH-PhIP. However, based on the control samples (Fig. 4Aa), this induction effect was negligible.

The transcription of many phase II enzymes is activated through Nrf2-antioxidant/electrophile response element (ARE) signaling pathway (11, 14, 51). After translocation into the nucleus, Nrf2 induces the expression of many cytoprotective proteins, including UGT1A isoforms. Therefore, we tested whether Nrf2 activation/nuclear translocation can be detected under SFN treatment. Indeed, Nrf2 was only stained in the cytoplasm of untreated cells whereas strong Nrf2 staining was present in the nuclei of SFN-treated cells, suggesting that SFN may induce UGT1A expression through the activation of Nrf2.

Except for Nrf2, several other ligand-activated transcription factors regulate phytochemical induction of UGTs, including the aryl hydrocarbon receptor (AhR), constitutive androstane receptor (CAR), peroxisome proliferator-activated receptor α (PPARα) and pregnane X receptor (PXR) (6). Some UGT1A isforms , such as UGT1A1, UGT1A3, UGT1A4 and UGT1A6 can be inducible *via* PXR-specific ligands (39). Interestingly, it has also been reported that SFN is a specific antagonist of human PXR (hPXR) and inhibited hPXR-mediated CYP3A4 drug clearance (53). It is interest to further dissect the mechanism of hPXR on induction of UGTs by SFN.

Furthermore, we found time- and dose-dependent antiproliferative effects of SFN in Caco-2 cells, consistent with observations made in other cancer cell types, including prostate cancer DU145 cells (9), Barrett's adenocarcinoma cells (38), human bladder cancer T24 cells (40), and human colon cancer HT-29 cells (41). We observed cell cycle arrest in Caco-2 cells treated with 25-100 μM SFN and IC50 was determined to be 50 μM (Fig. 1). SFN treatment resulted in the accumulation of Caco-2 cells at the G0/G1 phase (Table 2), consistent with observations in Barrett's adenocarcinoma FLO-1 and OE33 cells (38), human bladder cancer T24 cells, and human colon cancer (HT-29) cells (41). In contrast, a G2/M cell cycle arrest is more commonly seen after exposure of prostate cancer cells to SFN, including DU145 prostate cancer cells (9) and LNCaP human prostate cancer cell line (45). Notably, under SFN treatment, G2/M arrest is induced in human colon cancer HT-29 cells

through high-level expression of cyclin A and B1 (15) and in Caco-2 cells through the activation of the PI3K/Akt and MEK/ERK signaling pathways (21). Several potential mechanisms have been implicated in SFN-induced G0/G1 and G2/M cell cycle arrests, including increased expression of p21CIP1, generation of reactive oxygen species, activation of c-Jun N-terminal kinase signaling, checkpoint kinase 2-mediated phosphorylation of Cdc25C, inhibition of histone deacetylase, and decreased expression of cyclin D1 (9, 18).

As another piece of evidence supporting the antiproliferative effects of SFN, high concentrations of SFN (50-100 μM) were shown to induce apoptosis in Caco-2 cells (Fig. 6 and Table 2). This apoptosis-induction concentration range is consistent with findings from previous studies using human ovarian cancer cell SKOV3 cells (8) and hepatoblastoma HepG2-C8 cells (27). SFN at higher concentrations than 10 to 35 μM was reported to induce apoptosis in most cell lines, including colon cell line HT-29 (15), human U251 and U87 glioma cells (22), and prostate cancer cell line LNCaP (45). The SFN concentration necessary to induce apoptosis is even lower (at 3-7 μM) in Barrett's adenocarcinoma cell lines FLO-1 and OE33 (38). This discrepancy may reflect that different cell lines show a wide range of sensitivity towards SFN.

We further demonstrated that SFN induced apoptosis *via* decreasing the expression of the anti-apoptotic bcl-2 gene and increasing the expression of the apoptosis-inducing bax. Consistent with our observation, this mechanism of SFN-induced apoptosis has been elucidated in colon cancer cell line HT-29 cells (41), human U251, U87 glioma cells, HEK293 cells (22), and prostate cancer DU145 cells (9). Accordingly, a pro-apoptotic caspase-3 signaling pathway activated by bax is believed to represent, at least in part, regulatory pathways leading to SFN-induced apoptosis. Besides, sulforaphane has been reported to induce Ca^{2+}-independent cell death (42). However, because of multiple targets of SFN and complicated networks of cellular signaling pathways, the mechanisms of how SFN induces apoptosis still require future studies.

Epidemiologic studies have concluded that consumption of cruciferous vegetables reduces the risk of several types of cancers (19). However, it is difficult to reconcile this reduction in risk with current knowledge of sulforaphane metabolism, in which sulforaphane, after absorption, is found at relatively low concentrations in the plasma and is rapidly excreted. The peak plasmatic concentration of unconjugated SFN in human subjects who ingest SFN in broccoli can reach 2 to 3 μM, 24-h concentration is approximately 0.1 to 0.2 μM (16). Therefore, it is necessary to study the potential synergy of SFN combined with other phytochemicals or conventional chemotherapy to enhance its antineoplastic effect, and radiotherapy may also be considered (26). Srivastava *et al*. (44) have suggested that SFN, in combination with quercetin, can inhibit self-renewal capacity of pancreatic cancer stem cells. Herman-Antosiewicz (17) and Takeshi Nishikawa (35) demonstrated 3-methyladenine, an inhibitor of autophagy, could potentiates SFN-induced apoptosis in prostate cancer cells and colon cancer cells, respectively. These studies have provided promising research directions on SFN.

In summary, we propose that SFN at low concentrations may modulate nuclear translocation/activation of Nrf2 and then induce the transcription of defensive enzymes including phase II detoxifying enzymes, such as UGTs, leading to homeostatic protection of cells and tissues against exogenous and/or endogenous carcinogens. At concentrations higher than levels achieved by vegetable consumption (43), SFN may activate the caspase pathways and induce apoptosis, a potentially beneficial effect if occurring at preneoplastic/neoplastic tissues. Our data offer evidences that SFN could be applied in colon cancer prevention and treatment. Further assays are necessary to understand the chemosensitivity, safety, and cancer-preventive efficacy of SFN *in vivo*. New chemical substances which could potentiate antineoplastic effects of SFN also need further exploration.

Acknowledgments

This work was supported by grants from Science Bonus Funds for Young Scientists of Shandong Province (NO.2007BS03017), and Natural Science Foundation of Shandong Province (No.Y2008C115).

References

1. Alema, G., Yoko, O., Walle, U.K. and Walle, T. Induction of UDP- Glucuronosyltransferase UGT1A1 by the flavonoid chrysin in Caco-2 cells-potential role in carcinogen bioinactivation. *Pharm. Res*. 18: 374-379, 2001.
2. Ambrosone, C.B., McCann, S.E., Freudenheim, J.L., Marshall, J.R., Zhang, Y. and Shields, P.G. Breast cancer risk in premenopausal women is inversely associated with consumption of broccoli, a source of isothiocyanates, but is not modified by GST genotype. *J. Nutr*. 134: 1134-1138, 2004.
3. Ashok, B.T. and Tiwari, R.K. Cruciferous vegetables and cancer chemoprevention. *Recent Res. Dev. Nutr*. 6: 83-94, 2004.
4. Basten, G.P., Bao, Y. and Williamson, G. Sulforaphane and its glutathione conjugate but not sulforaphane nitrile induce UDP-glucuronosyl transferase (UGT1A1) and glutathione transferase (GSTA1) in cultured cell. *Carcinogenesis* 23: 1399-1404, 2002.
5. Bonnesen, C., Eggleston, I.M. and Hayes, J.D. Dietary indoles and isothiocyanates that are generated from cruciferous vegetables can both stimulate apoptosis and confer protection against DNA damage in human colon cell lines. *Cancer Res*. 61: 6120-6130, 2001.

6. Buckley, D.B. and Klaassen, C.D. Induction of mouse UDP-glucuronosyltransferase mRNA expression in liver and intestine by activators of aryl-hydrocarbon receptor, constitutive androstane receptor, pregnane X receptor, peroxisome proliferator-activated receptor α, and nuclear factor erythroid 2-related factor 2. *Drug Metab. Dispos*. 37: 847-856, 2009.
7. Campas-Baypoli, O.N., Sanchez-Machado, D.I., Bueno-Solano, C., Ramirez-Wong, B. and Lopez-Cervantes, J. HPLC method validation for measurement of sulforaphane level in broccoli by-products. *Biomed. Chromatogr*. 24: 387-392, 2010.
8. Chaudhuri, D., Orsulic, S. and Ashok, B.T. Antiproliferative activity of sulforaphane in Akt-overexpressing ovarian cancer cells. *Mol. Cancer Ther*. 6: 334-345, 2007.
9. Cho, S.D., Li, G., Hu, H., Jiang, C., Kang, K.S., Lee, Y.S., Kim, S.H. and Lu, J. Involvement of c-Jun N-terminal kinase in G2/M arrest and caspase-mediated apoptosis induced by sulforaphane in DU145 prostate cancer cells. *Nutr. Cancer* 52: 213-224, 2005.
10. Chung, F.L., Conaway, C.C., Rao, C.V. and Reddy, B.S. Chemoprevention of colonic aberrant crypt foci in Fischer rats by sulforaphane and phenethyl isothiocyanate. *Carcinogenesis* 21: 2287-2291, 2000.
11. Dinkova-Kostova, A.T., Massiah, M.A., Bozak, R.E., Hicks, R.J. and Talalay, P. Potency of Michael reaction acceptors as inducers of enzymes that protect against carcinogenesis depends on their reactivity with sulfhydryl groups. *Proc. Natl. Acad. Sci. USA* 98: 3404-3409, 2001.
12. Evans, W.E. and Relling, M.V. Pharmacogenomics: translating functional genomics into rational therapeutics. *Science* 286: 487-491, 1999.
13. Fahey, J.W., Haristoy, X., Dolan, P.M., Kensler, T.W., Scholtus, L., Stephenson, K.K., Talalay, P. and Lozniewski, A. Sulforaphane inhibits extracellular, intracellular, and antibiotic-resistant strains of *Helicobacter pylori* and prevents benzo[*a*]pyrene-induced stomach tumors. *Proc. Natl. Acad. Sci. USA* 99: 7610-7615, 2002.
14. Faulkner, K., Mithen, R. and Williamson, G. Selective increase of the potential anticarcinogen 4-methylsulphinylbutyl glucosinolate in broccoli. *Carcinogenesis* 19: 605-609, 1998.
15. Gamet- Payrastre, L., Li, P., Lumeau, S., Cassar, G., Dupont, M.A., Chevolleau, S., Gasc, N., Tulliez, J. and Terce, F. Sulforaphane, a naturally occurring isothiocyanate induces cell cycle arrest and apoptosis in HT29 human colon cancer cells. *Cancer Res*. 60: 1426-1433, 2000.
16. Gasper, A.V., Al-Janobi, A., Smith, J.A., Bacon, J.R., Fortun, P., Atherton, C., Taylor, M.A., Hawkey C.J., Barrett, D.A. and Mithen, R.F. Glutathione S-transferase M1 polymorphism and metabolism of sulforaphane from standard and high-glucosinolate broccoli. *Am. J. Clin. Nutr*. 82: 1283-1291, 2005.
17. Herman-Antosiewicz, A., Johnson, D.E. and Singh, S.V. Sulforaphane causes autophagy to inhibit release of cytochrome c and apoptosis in human prostate cancer cells. *Cancer Res*. 66: 5828-5835, 2006.
18. Herman-Antosiewicz, A., Xiao, H., Lew, K.L. and Singh, S.V. Induction of p21 protein protects against sulforaphane-induced mitotic arrest in LNCaP human prostate cancer cell line. *Mol. Cancer Ther*. 6: 1673-1681, 2007.
19. Higdon, J.V., Delage, B., Williams, D.E. and Dashwood, R.H. Cruciferous vegetables and human cancer risk: epidemiologic evidence and mechanistic basis. *Pharmacol. Res*. 55: 224-236, 2007.
20. Husoy, T., Syverson, T. and Jenssen, J. Comparison of four *in vitro* cytotoxicity tests: the MTT assay, NR assay, uridine incorporation and protein measurements. *Toxicol. In Vitro*. 7: 149-154, 1993.
21. Jakubikova, J., Sedlak, J., Mithen, R. and Bao, Y. Role of PI3K/Akt and MEK/ERK signaling pathways in sulforaphane- and erucin-induced phase II enzymes and MRP2 transcription, G2/M arrest and cell death in Caco-2 cells. *Biochem. Pharmacol*. 69: 1543-1552, 2005.
22. Jiang, H., Shang, X., Wu, H., Huang, G., Wang, Y., Al-Holou, S., Gautam, S.C. and Chopp, M. Combination treatment with resveratrol and sulforaphane induces apoptosis in human U251 glioma cells. *Neurochem. Res*. 35: 152-161, 2010.
23. Johansson, N.L., Pavia, C.S. and Chiao, J.W. Growth inhibition of a spectrum of bacterial and fungal pathogens by sulforaphane, an isothiocyanate product found in broccoli and other cruciferous vegetables. *Planta Med*. 74: 747-750, 2008.
24. Joseph, M.A., Moysich, K.B., Freudenheim, J.L., Shields, P.G., Bowman, E.D., Zhang, Y., Marshall, J.R. and Ambrosome, C.B. Cruciferous vegetables, genetic polymorphisms in glutathione S-transferases M1 and T1, and prostate cancer risk. *Nutr. Cancer* 50: 206-213, 2004.
25. Karmakar, S., Banik, N.L., Patel, S.J. and Ray, S.T. Curcumin activated both receptor-mediated and mitochondria-mediated proteolytic pathways for apoptosis in human glioblastoma T98G cells. *Neurosci. Lett*. 407: 53-58, 2006.
26. Kiang, J.G., Garrison, B.R. and Gorbunov, N.V. Radiation combined injury: DNA damage, apoptosis, and autophagy. *Adapt. Med*. 2: 1-10, 2010.
27. Kim, B.R., Hu, R., Keum, Y.S., Hebbar, V., Shen, G., Nair, S.S. and Kong, A.N. Effects of glutathione on antioxidant response element-mediated gene expression and apoptosis elicited by sulforaphane. *Cancer Res*. 63: 7520-7525, 2003.
28. Lin, H.J., Probst-Hensch, N.M., Louie, A.D., Kau, I.H., Witte, J.S., Ingles, S.A., Frankl, H.D., Lee, E.R. and Haile, R.W. Glutathione transferase null genotype, broccoli and lower prevalence of colorectal adenomas. *Cancer Epidemiol. Biomark. Prev*. 7: 647-652, 1998.
29. Lin, W., Wu, R.T., Khor, T.O., Wang, H. and Kong, A.N. Sulforaphane suppressed LPS-induced inflammation in mouse peritoneal macrophages through Nrf2 dependent pathway. *Biochem. Pharmacol*. 76: 967-973, 2008.
30. Maheo, K., Morel, F., Langouet, S., Kramer, H., Le Ferrec, E., Ketterer, B. and Guillouzo, A. Inhibition of cytochromes P-450 and induction of glutathione *S*-transferases by sulforaphane in primary human and rat hepatocytes. *Cancer Res*. 57: 3649-3652, 1997.
31. Marc, A., Riedl, M.S., Andrew, S. and David, D.S. Oral Sulforaphane increases phase II antioxidant enzymes in the human upper airway. *Clin. Immunol*. 130: 244-251, 2009.
32. Michael, A.M. and James, S.F. N-Glucuronidation of 2-amino-1-methyl-6 -phenylimidazo [4,5-b]pyridine (PhIP) and N-hydroxy-PhIP by specific human UDP-glucuronosyltransferases. *Carcinogenesis* 22: 1087-1093, 2001.
33. Morimitsu, Y., Nakagawa, Y., Hayashi, K., Fujii, F., Kumagai, T., Nakamura, Y., Osawa, T., Horio, F., Itoh, K., Lida, K., Yamamoto, M. and Uchida, K. A sulforaphane analogue that potently activates the Nrf2-dependent detoxification pathway. *J. Biol. Chem*. 277: 3456-3463, 2002.
34. Munzel, P., Bookjans, G., Mehner, G., Lehmkoster, T. and Bock, K. Tissue-specific 2,3,7,8-tetrachlorodibenzo-p-dioxin-inducible expression of human UDP-glucuronosyltransferase UGT1A6. *Arch. Biochem. Biophys*. 335: 205-210, 1996.
35. Nishikawa, T., Tsuno, N.H., Okaji, Y., Shuno, Y., Sasaki, K., Hongo, K., Sunami, E., Kitayama, J., Takahashi, K. and Nagawa, H. Inhibition of autophagy potentiates sulforaphane-induced apoptosis in human colon cancer cells. *Ann. Surg. Oncol*. 17: 592-602, 2010.
36. Nowell, S.A., Massengill, J.S., Williams, S., Radominska-Pandya, A., Tephly, T.R., Cheng, Z., Strassburg, C.P., Tukey, R.H., MacLeod, S.L., Lang, N.P. and Kadlubar, F.F. Glucuronidation of 2-hydroxyamino-1-methyl-6-phenylimidazo [4,5-^{b}]pyridine by human microsomal UDP-glucuronosyltransferases: identification of specific UGT1A family isoforms involved. *Carcinogenesis* 20: 1107-1114, 1999.
37. Petri, N., Tannergren, C., Holst, B., Mellon, F.A., Bao, Y., Plumb, G.W., Bacon, J., O'Leary, K.A., Kroon, P.A., Knutson, L., Forsell, P., Eriksson, T., Lennernas, H. and Williamson, G. Absorption/metabolism of sulfapaphane and quercetin, and regulation of phase II enzymes, in human jejunum *in vivo*. *Drug Metab. Dispos*. 31:

805-813, 2003.

38. Qazi, A., Pal, J., Maitah, M., Fulciniti, M., Pelluru, D., Nanjappa, P., Batchu, R.B., Prasad, M., Bryant, C.S., Raiput, S., Lee, S., Anderson, K.C., Gryaznov, S., Beer, D.G., Weaver, D.W., Munshi, N.C., Goyal, R.K. and Shammas, M.A. Anticancer activity of a broccoli derivative, sulforaphane, in Barrett's adenocarcinoma: Potential use in chemoprevention and as adjuvant in chemotherapy. *Gastroenterology* 138 (Supplement 1): S-500, 2010.
39. Saracino, M.R. and Lampe, J.W. Phytochemical regulation of UDP-glucuronosyltransferases: implications for cancer prevention. *Nutr. Cancer* 59: 121-141, 2007.
40. Shan, Y., Sun, C., Zhao, X., Wu, K., Cassidy, A. and Bao,Y. Effect of sulforaphane on cell growth, G_0/G_1 phase cell progression and apoptosis in human bladder cancer T24 cells. *Int. J. Oncol*. 29: 883-888, 2006.
41. Shen, G., Xu, C., Chen, C., Hebbar, V. and Kong, A.N. p53-Independent G1 cell cycle arrest of human colon carcinoma cells HT-29 by sulforaphane is associated with induction of p21CIP1 and inhibition of expression of cyclin D1. *Cancer Chemother Pharmacol*. 57: 317-327, 2006.
42. Shieh, P., Tsai, M.L., Chiu, M.H., Chen, Y.O., Yi, N.L. and Jan, C.R. Independent effects of the broccoli-derived compound sulforaphane on Ca^{2+} influx and apoptosis in madin-darby canine renal tubular cells. *Chinese J. Physiol*. 53: 215-222, 2010.
43. Song, L.J., Morrison, J.J., Botting, N.P. and Thornalley, P.J. Analysis of glucosinolates, isothiocyanates, and amine degradation products in vegetable extracts and blood plasma by LC-MS/MS. *Anal Biochem*. 347: 234-243, 2005.
44. Srivastava, R.K., Tang, S.N., Zhu, W., Meeker, D. and Shankar, S. Sulforaphane synergizes with quercetin to inhibit self-renewal capacity of pancreatic cancer stem cells. *Front Biosci (Elite Ed)*. 3: 515-528, 2011.
45. Suvarna, B., Sahoo, D., Tibshirani, R., Dill, D.L. and Brooks, J.D. Temporal changes in gene expression induced by sulforaphane in human prostate cancer cells. *Prostate* 69: 181-190, 2009.
46. Thejass, P. and Kuttan, G. Modulation of cell-mediated immune response in B16F-10 melanoma-induced metastatic tumor-bearing C57BL/6 mice by sulforaphane. *Immunopharmacol. Immunotoxicol*. 29: 173-186, 2007.
47. Van Poppel, G., Verhoeven, D.T.H., Verhagen, H. and Goldbohm, R.A. Brassica vegetables and cancer prevention. Epidemiology and mechanisms. *Adv. Exp. Med. Biol*. 472: 159-168, 1999.
48. Wan, D.S. Epidemiologic trend of and strategies for colorectal cancer. *Chinese J. Cancer* 28: 897-902, 2009.
49. Wang, M., Li, Y.Q., Chen, J., Liu, F.G., Liu, H.T., Xu, X.Q. and Yuan, M.B. Polymorphic gene regulation of UDP-glucuronosyltransferase 1A in human colorectal epithelium and liver. *Chinese J. Dig*. 26: 96-99, 2006.
50. Xu, C., Huang, M.T., Shen, G., Yuan, X.L., Lin, W., Khor, T.O., Conney, A.H. and Kong, A.N.T. Inhibition of 7,12-dimethylbenz (*a*)anthracene-induced skin tumorigenesis in C57BL/6 mice by sulforaphane is mediated by nuclear factor E2-related factor 2. *Cancer Res*. 66: 8293-8296, 2006.
51. Zhang, Y. and Gordon, G.B. A strategy for cancer prevention: stimulation of the Nrf2-ARE signaling pathway. *Mol. Cancer Ther*. 3: 885-893, 2004.
52. Zhang, Y., Talalay, P., Cho, C.G. and Posner, G.H. A major inducer of anticarcinogenic protective enzymes from broccoli: isolation and elucidation of structure. *Proc. Natl. Acad. Sci. USA* 89: 2399-2403, 1992.
53. Zhou, C., Poulton, E.J., Grün, F., Bammler, T.K., Blumberg, B., Thummel, K.E. and Eaton, D.L. The dietary isothiocyanate sulforaphane is an antagonist of the human steroid and xenobiotic nuclear receptor. *Mol. Pharmacol*. 71: 220-229, 2007.